Since January 2020 Elsevier has created a COVID-19 resource centre with free information in English and Mandarin on the novel coronavirus COVID-19. The COVID-19 resource centre is hosted on Elsevier Connect, the company's public news and information website.

Molecular Therapy
Original Article

Debulking SARS-CoV-2 in saliva using angiotensin converting enzyme 2 in chewing gum to decrease oral virus transmission and infection

Henry Daniell,[1] Smruti K. Nair,[1,6] Nardana Esmaeili,[1,6] Geetanjali Wakade,[1] Naila Shahid,[1] Prem Kumar Ganesan,[1] Md Reyazul Islam,[1] Ariel Shepley-McTaggart,[3] Sheng Feng,[2] Ebony N. Gary,[4] Ali R. Ali,[4] Manunya Nuth,[1] Selene Nunez Cruz,[2] Jevon Graham-Wooten,[2] Stephen J. Streatfield,[5] Ruben Montoya-Lopez,[5] Paul Kaznica,[5] Margaret Mawson,[5] Brian J. Green,[5] Robert Ricciardi,[1] Michael Milone,[2] Ronald N. Harty,[3] Ping Wang,[2] David B. Weiner,[4] Kenneth B. Margulies,[2] and Ronald G. Collman[2]

[1]Department of Basic and Translational Sciences, School of Dental Medicine, University of Pennsylvania, Philadelphia, PA 19104, USA; [2]Department of Medicine, University of Pennsylvania Perelman School of Medicine, Philadelphia, PA 19104, USA; [3]Department of Pathobiology, School of Veterinary Medicine, University of Pennsylvania, Philadelphia, PA 19104, USA; [4]The Wistar Institute, 3601 Spruce Street, Philadelphia, PA 19104, USA; [5]Fraunhofer USA, Center Mid-Atlantic, Newark, DE 19711, USA

To advance a novel concept of debulking virus in the oral cavity, the primary site of viral replication, virus-trapping proteins CTB-ACE2 were expressed in chloroplasts and clinical-grade plant material was developed to meet FDA requirements. Chewing gum (2 g) containing plant cells expressed CTB-ACE2 up to 17.2 mg ACE2/g dry weight (11.7% leaf protein), have physical characteristics and taste/flavor like conventional gums, and no protein was lost during gum compression. CTB-ACE2 gum efficiently (>95%) inhibited entry of lentivirus spike or VSV-spike pseudovirus into Vero/CHO cells when quantified by luciferase or red fluorescence. Incubation of CTB-ACE2 microparticles reduced SARS-CoV-2 virus count in COVID-19 swab/saliva samples by >95% when evaluated by microbubbles (femtomolar concentration) or qPCR, demonstrating both virus trapping and blocking of cellular entry. COVID-19 saliva samples showed low or undetectable ACE2 activity when compared with healthy individuals (2,582 versus 50,126 ΔRFU; 27 versus 225 enzyme units), confirming greater susceptibility of infected patients for viral entry. CTB-ACE2 activity was completely inhibited by pre-incubation with SARS-CoV-2 receptor-binding domain, offering an explanation for reduced saliva ACE2 activity among COVID-19 patients. Chewing gum with virus-trapping proteins offers a general affordable strategy to protect patients from most oral virus re-infections through debulking or minimizing transmission to others.

INTRODUCTION

SARS-CoV-2 transmission occurs through both droplet and aerosol transmission and is linked in large part with indoor exposure of infected individuals, symptomatic or asymptomatic. Controlling transmission has involved reduction of concentrations of indoor aerosols largely through masking and physical distancing. In public buildings (e.g., classrooms, retail shops, restaurants, gyms, churches), air exchanges through filters to decrease transmission.[1] Most people emit >100 times smaller aerosols (<5 μm) during talking, breathing, or coughing.[2] Less than 10% of the global population is currently vaccinated, only to be made worse by the shortage of the SARS-CoV-2 vaccines and evolving new strains with higher viral load and greater transmission.[3–8] With >200 million confirmed infections and 5 million deaths and the pandemic still out of control in several countries around the globe, there is impetus to develop measures to decrease the transmission and infection of SARS-CoV-2.

A high SARS-CoV-2 viral load is often detected in saliva.[9] Highly contagious airborne droplets are the major cause of transmission in respiratory viruses such as influenza, measles, and SARS-CoV-2.[10–13] Human papillomavirus, herpes simplex virus type 1, Epstein-Barr virus, and Kaposi's sarcoma-associated herpesvirus are orally transmitted, and their life cycle in the oral epithelium is well known.[14,15] In SARS-CoV-2 with saliva average load of 7×10^6 copies of RNA virus per milliliter, an oral fluid droplet of 50 μm^2 could contain at least one virion.[2,14] High SARS-CoV-2 viral loads are detected in saliva of both asymptomatic and symptomatic COVID-19 patients.[16,17] In fact, salivary viral burden correlates with the severity of COVID-19 symptoms including the loss of taste and smell, and the virus replicates in salivary glands and oral mucous membranes.[18] Thus, the oral mucous membranes and saliva appear] to be a high-risk route for SARS-CoV-2 transmission, and viral inactivation within the

Received 1 November 2021; accepted 7 November 2021;
https://doi.org/10.1016/j.ymthe.2021.11.008.

[6]These authors contributed equally

Correspondence: Dr. Henry Daniell, W.D. Miller Professor, Vice-Chair, Department of Basic and Translational Sciences, University of Pennsylvania, 240 South 40th Street, 547 Levy Building, Philadelphia, PA 19104-6030, USA.
E-mail: hdaniell@upenn.edu

Please cite this article in press as: Daniell et al., Debulking SARS-CoV-2 in saliva using angiotensin converting enzyme 2 in chewing gum to decrease oral virus transmission and infection, Molecular Therapy (2021), https://doi.org/10.1016/j.ymthe.2021.11.008

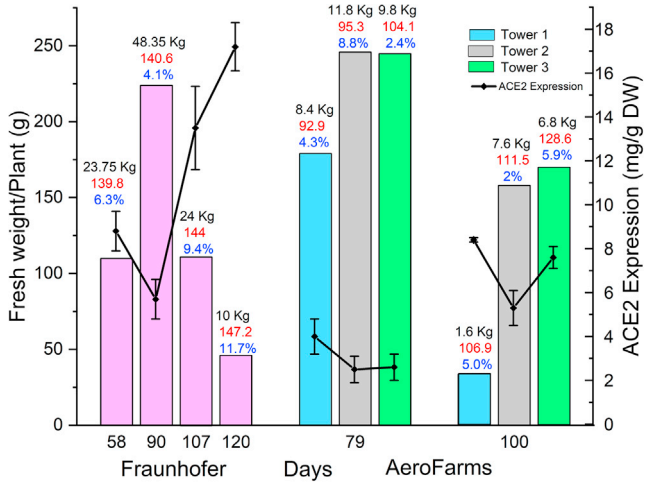

Figure 1. Fresh weight per plant (g) and ACE2 expression (mg/g dry weight) at different ages between AeroFarms and Fraunhofer

The ACE2 expression was quantified based on total protein of homogenate (μg/μL) and converted to mg/g of plant dried weight (mg/g DW).The values are mean ± SD (n = 3).The percentage of ACE2 protein content in total leaf protein is presented on top of each column in blue. Total leaf protein content (mg/g DW) of CTB-ACE2 plant material is presented on top of each column in red. The values are the mean ± SD (n = 8). Total fresh biomass (kg) harvested at different ages is presented on top of each column in black. Plant ages are relative to the date of germination.

oral cavity could be an important strategy to reduce viral infectivity at source.

COVID-19 patients have low angiotensin-converting enzyme 2 (ACE2) activity due to renin-angiotensin-aldosterone dysregulation, which causes respiratory stress,[19–21] and injected ACE2 restores health in COVID-19 patients.[22] ACE receptor traps have large binding interfaces capable of blocking the entire receptor interface, thereby facilitating inhibition of different SARS-CoV-1 and SARS-CoV-2 variants.[23,24] In the absence of any Food and Drug Administration (FDA) approved receptor traps as antiviral biologics,[25] several traps using soluble ACE2 as nasal spray have been recently developed.[23] While nasal sprays could help in reducing viral load in the nose, additional approaches are needed to decrease viral load in saliva because salivary glands are the primary sites of SARS-CoV-2 replication.[9,17,18] That salivary glands serve as a reservoir of replication for viruses causing highly prevalent diseases such as Epstein-Barr virus, herpes simplex, HHV-7, cytomegalovirus, hepatitis C, and Zika virus is a known fact.[26–29] Newly evolving strains have higher viral load in saliva and greater transmission.[4–7] The viral load of people infected by the delta variant is 1,260 times higher than in individuals infected with previous strains.[4] The Centers for Disease Control and Prevention have reported a higher basic reproduction rate (R0) of 5–8 for the delta variant, which estimates to 60,466,176 infections as opposed to R0 of 2.79 of the ancestral strain,[30] which translates to an estimated 9,536 infections.[31] The delta variant is 40%–60% more contagious than the previously dominant alpha strain.[31,32] High viral density and transmissibility of these variants, along with the increase in replication potential and serial viral shedding,[33] warrants development of novel approaches to curb viral loads in saliva.

Mouthwashes with antimicrobial agents have a short period of contact.[32] Therefore, in this study we explore longer duration of contact using the chewing gum topical delivery approach. SARS-CoV-2 utilizes ACE2 and GM1 co-receptors to enter human cells.[34–38] Therefore, in this study we explore receptor binding/blocking proteins cholera toxin B (CTB)-ACE2 chewing gum to minimize transmission and decrease infectivity by binding directly to the spike protein to trap virus particles and saturate both ACE2/GM1 receptors located in close proximity on the surface of human oral epithelial cells. Furthermore, we explore the impact of SARS-CoV-2 on ACE2 activity in saliva and its potential role as biomarker to distinguish symptomatic from asymptomatic COVID-19 patients. In addition to prophylactic protection against COVID in general social settings or restaurants, the ACE2 gum could be used as a rapid means of reducing SARS-CoV-2 from the oral cavity of infected patients requiring dental procedures. This general concept could be extended to minimize infection or transmission of most oral viruses.

RESULTS

Clinical-grade ACE2 plant biomass production at Fraunhofer USA and AeroFarms

CTB-ACE2 plants were created as reported in a previous publication.[43] Seeds from the same batch were grown at Fraunhofer USA and AeroFarms as described in materials and methods. While growth conditions were different, biomass yield per plant was similar at 80–90 days and declined with repeated harvests as plants grew older. However, total biomass harvested decreased dramatically at Fraunhofer from 48.3 kg on day 90 to 10 kg on day 120. At AeroFarms, total biomass decreased in tower 1 (higher far-red light) from 8.4 kg on day 79 to 1.6 on day 100, but two other towers (higher blue light) showed a moderate decrease in biomass (Figure 1 and Table 1). Biomass yields at Fraunhofer and AeroFarms (towers 2 and 3) were very similar based on fresh weight. Expression level of CTB-ACE2 was higher at Fraunhofer (17.2 ± 1.1 mg/g dry weight [DW] or 11.7% ACE2 in total leaf protein [TLP]), a significant improvement from a previous report[43] achieved by optimizing growth conditions, including increasing spacing and light intensity. At AeroFarms, tower 1 with higher far-red percentage showed higher expression (8.4 ± 0.1 mg/g DW or 8.8% TLP) than the other two towers. The reproducibility of ACE2 protein expression was evaluated in several independent trials of plants grown at Fraunhofer and AeroFarms, the statistical data of which is presented in Table 1. However, irrespective of growth conditions, the highest expression was observed in the oldest plants when the lowest biomass was harvested at both facilities (Figure 1 and Table 1). Therefore, delayed single final harvest could further improve protein drug production and yield. Total protein based on dry weight was also higher at Fraunhofer (140–147 mg/g DW) than plants grown at AeroFarms (93–129 mg/g DW), suggesting that the different nutrient solutions influence protein synthesis (Figures 1 and S1; Table 1). Higher level expression reduces the

Table 1. Fresh harvested biomass, moisture content, total protein content, and ACE2 content of CTB-ACE2 plants grown at Fraunhofer and AeroFarms related to their age and growth condition

Entity	Growth condition	Age (days)	Fresh weight/ plant (g)	Total fresh biomass (kg)	Moisture content (%)	CTB-ACE2 expression (mg/g DW) ± SD	Total protein content (mg/g DW) ± SD	% CTB-ACE2 content/total protein content
Fraunhofer	standard	58	110	23.8	5.6	8.8 ± 0.9	139.8 ± 4.2	6.3
		90	224	48.4	10.9	5.7 ± 0.9	140.6 ± 6.6	4.1
		107	111	24	7.4	13.5 ± 1.9	144.0 ± 7.6	9.4
		120	46	10	6.98	17.2 ± 1.1	147.2 ± 6.0	11.7
AeroFarms	tower 1	79	179	8.4	5.6–6.3	4.0 ± 0.8	92.9 ± 1.5	4.3
		100	34	1.6	6.2	8.4 ± 0.1	95.3 ± 2.3	8.8
	tower 2	79	245	11.8	7.4	2.5 ± 0.6	104.1 ± 6.7	2.4
		100	158	7.6	5.3	5.3 ± 0.8	106.9 ± 5.6	5.0
	tower 3	79	245	9.8	6.5	2.6 ± 0.6	111.5 ± 6.8	2.3
		100	170	6.8	5.6	7.6 ± 0.5	128.6 ± 5.0	5.9

The values of CTB-ACE2 expression are mean ± SD (n = 3). The values for total leaf protein are the mean ± SD (n = 8).

amount of plant powder required for chewing gum or oral delivery of therapeutic ACE2 and therefore is an important production metric.

Preparation of chewing gums

Chewing gum tablets containing ground plant powder were prepared by Per Os Biosciences (Hunt Valley, MD) by a compression process but not the traditional gum manufacturing process, which requires higher temperature and extrusion/rolling that introduces variability in the concentration of proteins. Placebo gum tablets contained the gum base (28.2%), maltitol (20.4%), sorbitol (13%), xylitol (13%), isomalt (13%), natural and artificial flavors, magnesium stearate (3%), silicon dioxide (0.43%), and stevia (0.65%) in order to offer the best flavor, taste, softness, and compression. The gum tablet (2 g weight) chews and performs exactly like conventional chewing gum based on physical characteristics. Freeze-dried plant cells were ground with five pulses to disrupt plant cells and readily release CTB-ACE2. The ACE2 gum tablet has all the components of the placebo gum but in addition includes 50 mg of CTB-ACE2 freeze-dried 5× ground plant cells. Evaluation of sum total of proteins in all fractions (supernatant and pellet) revealed an insignificant loss of CTB-ACE2 during the gum manufacturing process (Figure S2).

Debulking and blocking of viral entry using ACE2 chewing gum

CTB has been shown to be a transmucosal carrier and facilitates oral delivery of therapeutic proteins by forming a pentameric structure and binding to gut GM1 epithelial receptors.[43–46] CTB-ACE2 has the potential to effectively bind to both the GM1 and ACE2 receptor-binding sites located in close proximity on the human cell surface and thereby prevent viral entry into human cells, especially via oral epithelial cells that are enriched with both receptors.[47] In addition, direct binding of ACE2 to the SARS-CoV-2 spike proteins could trap the virus particles and decrease infectivity (Figure 2). Pentameric insoluble microparticles[43,44] of CTB-ACE2 could facilitate removal of bound viral particles by centrifugation. Therefore, CTB-ACE2 chewing gum is evaluated in this study for its impact on entry and transmission of SARS-CoV-2 (Figure 2). In the oral cavity, tongue epithelial cells constitute a large reservoir of ACE2, even more so than buccal and gingival tissues.[43–46] The ACE2 released upon mastication of the chewing gum serves as a novel approach to diminish virus infection.

Evaluation of SARS-CoV-2 in swab samples by microbubbles and gum

Several de-identified nasopharyngeal (NP) swab samples collected from patients positive for SARS-CoV-2 nucleic acid and nucleocapsid antigen were used to evaluate the neutralization of viral particles by ACE2 gum. The microbubble SARS-CoV-2 antigen assay detects the nucleocapsid antigen of SARS-CoV-2 at femtomolar concentration.[40,41] The number and size of microbubbles correlates with the amount of nucleocapsid antigen in the sample. Because of the limited volume of swab samples, a dose-dependent study on ACE2 gum could not be done using the same patient sample or in duplicates/triplicates. A dose-dependent study was therefore carried out using different patient samples. Samples of patient 1 and patient 2 were treated with 25 mg of gum per 150-μL sample, and the sample of patient 3 was treated with 50 mg of gum per 150-μL sample. Samples were then tested using the microbubble SARS-CoV-2 antigen assay. As shown in Figure 3, the incubation of swab samples with ACE2 gum significantly reduced the microbubble count ($p = 0.004$). In contrast, the placebo gum when compared with the untreated group had less significant variation ($p = 0.892$). ACE2 gum decreased the amount of nucleocapsid antigens in COVID-19 patient samples even at very low concentration (25 mg), whereas each gum weighs 2 g. These results confirm direct binding of ACE2 to the SARS-CoV-2 spike proteins and entrapment in pentameric insoluble microparticles of CTB-ACE2 facilitating removal of bound viral particles by centrifugation.

Neutralization assay with SARS-CoV-2 spike-pseudotyped lentiviral particles

CTB-ACE2 has the potential to effectively bind to both the GM1 and ACE2 receptor-binding sites located in close proximity on the human

Please cite this article in press as: Daniell et al., Debulking SARS-CoV-2 in saliva using angiotensin converting enzyme 2 in chewing gum to decrease oral virus transmission and infection, Molecular Therapy (2021), https://doi.org/10.1016/j.ymthe.2021.11.008

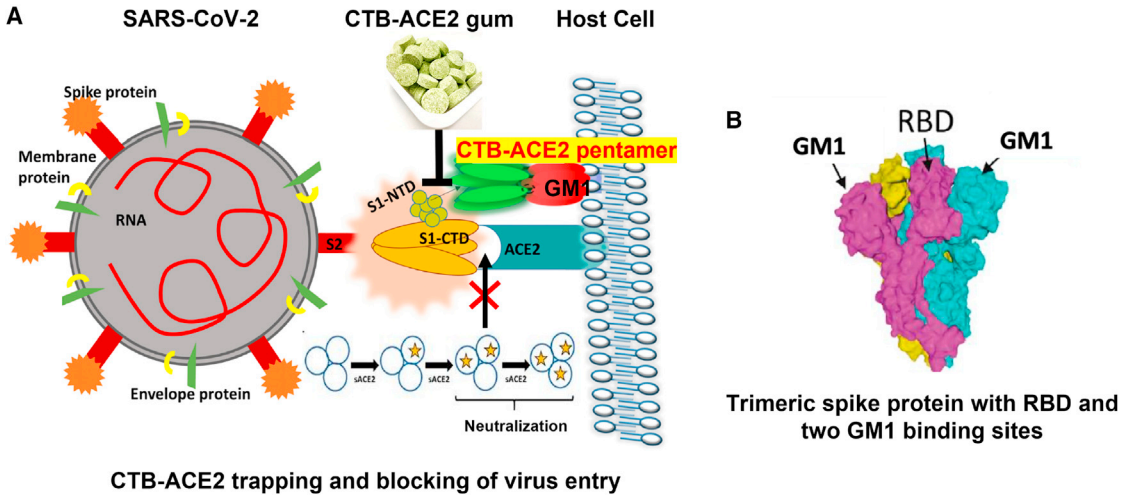

Figure 2. Debulking and blocking of viral entry using ACE2 chewing gum

(A) CTB-ACE2 binds to both ACE2 and GM1 co-receptors. (B) Each SARS-CoV2 trimeric spike protein has a single RBD domain and two GM1 binding sites. CTB-ACE2 pentamers form microparticles, insoluble and sediment SARS-CoV-2 upon binding to soluble ACE2, in monomer, dimer, or trimer forms. CTB-ACE2 also directly binds to ACE2 and GM1 receptors, thereby blocking entry into human or Vero cells.

cell surface and thereby prevent viral entry into human cells. Therefore, we employed a SARS-CoV-2 pseudotyped lentivirus (also referred to as lentivirus particles) to determine the effectiveness of ACE2 gum in neutralizing spike-mediated viral infection. Lentiviral particles pseudotyped with the viral spike protein and harboring the pseudoviruses expressing a luciferase reporter gene were used to infect Chinese hamster ovary (CHO) cells expressing human ACE2.[48] SARS-CoV-2 spike glycoprotein pseudotyped viruses expressing luciferase were incubated with ACE2 gum at the indicated concentration for 90 min at room temperature. Following centrifugation, virus-containing supernatant was incubated with ACE2-expressing CHO cells for 72 h, and viral infectivity was measured via luciferase. Data shown in Figure 4 are representative of three independent experiments (N = 2–3 samples). Bars represent the condition mean, symbols represent the average of duplicate or triplicate assays, and error bars represent the SEM. The incubation of pseudotyped lentivirus with increasing amounts of CTB-ACE2 gum significantly reduced luciferase activities in a dose-dependent manner: at 50 mg of CTB-ACE2 the highest inhibition ($p < 0.0001$) was observed (Figure 4), confirming the ability of this protein to block entry of lentivirus spike protein into CHO cells either by direct binding to the spike protein or by binding of CTB-ACE2 to ACE2/GM1 receptors on CHO cells.

VSV-S pseudotype entry is inhibited by recombinant CTB-ACE2 and ACE2 gum powder

The red fluorescent protein (RFP)-expressing vesicular stomatitis virus spike (VSV-S) pseudotype particles utilize the SARS-CoV-2 spike (S) protein to bind and enter cells. We investigated the impact of purified recombinant CTB-ACE2 protein or ACE2 gum powder binding to VSV-S particles and inhibition of viral particle entry into Vero cells. In repeated experiments, we observed that VSV-S entry was inhibited with the addition of CTB-ACE2 by approximately 85% when compared with untreated controls (Figure 5, lane 2), confirming the antiviral effect of our recombinant protein on entry of the VSV-S pseudotypes. We also observed a dose-dependent inhibition of entry when VSV-S particles were incubated with increasing concentrations of our ACE2 gum powder (Figure 5, lanes 3–6). Indeed, representative images from fluorescent microscopy highlight clear and significant differences in the number of cells expressing RFP in control versus 20-mg ACE2 gum powder samples (Figure S3). Taken together, these data show that CTB-ACE2 protein and ACE2 gum powder traps the VSV-S pseudotype particles, thus decreasing viral entry either by binding directly to the spike protein or by binding to ACE2/GM1 receptors on the surface of Vero cells.

ACE2 activity in healthy control and COVID-19 patient saliva

After informed consent under protocol #823392 approved by the University of Pennsylvania (UPenn) IRB, saliva samples were obtained from hospitalized patients with confirmed SARS-CoV-2 infection and healthy volunteers confirmed to be free of SARS-CoV-2 infection. Results on analysis of ten samples each of healthy and COVID-19 (PCR positive) are presented in Figure 6. ACE2 activity was markedly reduced in COVID-19 patients compared with controls (Figures 6A–6C). We observed a drastic reduction in ACE2 activity in viral-laden saliva collected from ten COVID-19 patients compared with healthy individuals (2,582 ± 439.82 versus 50,126 ± 2,102, change in relative fluorescence units [ΔRFU]: 27.63 ± 9.52 versus 225 ± 30.82 mU/mg enzyme activity units). The fluorescent cleaved product of ACE2 (Mca-YVADAPK) steadily increased up to 90 min in control saliva samples. While all COVID-19 saliva samples showed a similar low and almost undetectable ACE2 activity, one sample stood out as an outlier with enzyme activity (38,504 ± 9,688 ΔRFU; 236.4 ± 60.28 mU/mg enzyme activity units) similar to control

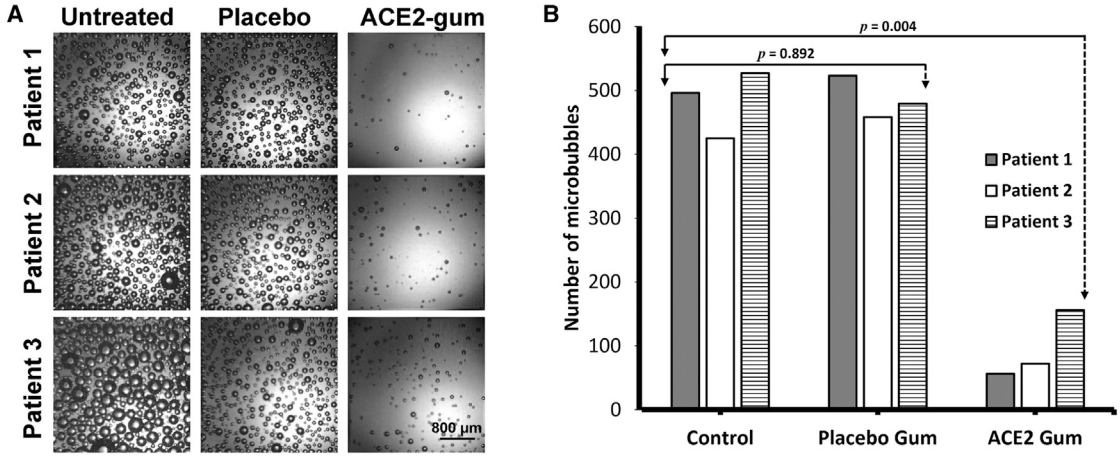

Figure 3. Neutralization of SARS-CoV-2 in NP swab samples

(A) Images from clinical NP swab samples treated with placebo or ACE2 gum. All images share the same scale bar. (B) The number of bubbles for various treatments are quantified. Patient 1 and patient 2 were treated by 25 mg of ACE2 gum per 100-µL sample, and patient 3 was treated by 50 mg of gum per 100-µL sample. Data were analyzed using the Student's t test. While no statistical significance was found between untreated and placebo gum ($p = 0.892$), significant difference was seen with the ACE2 gum-treated group ($p = 0.004$). Standard deviation could not be added to individual samples due to limited volume of COVID-19 patient swab samples to run duplicate or triplicate biological replicates for three treatment conditions.

saliva (Figures 6A and 6B). This patient was identified as SARS-CoV-2 positive through routine screening of hospital admissions and had no symptoms of COVID-19 infection, although PCR confirmed virus in the saliva.

The activity of CTB-ACE2 is inhibited by SARS-CoV-2 spike protein

To investigate the mechanism of decreased ACE2 activity observed in COVID-19 saliva, we performed *in vitro* enzymatic assays using plant extract containing full-length CTB-ACE2 in the presence or absence of the SARS-CoV-2 spike protein (receptor-binding domain [RBD] S1-S2). The fluorescent cleaved product of CTB-ACE2 protein extracts (Mca-YVADAPK) increased up to 90 min, demonstrating that ACE2 was enzymatically active (Figure 6D). However, this activity was partially inhibited when CTB-ACE2 was pre-incubated with 10 µg of SARS CoV-2 S1-S2 spike protein for 30 min at room temperature (Figure 6D). In fact, ACE2 activity showed complete inhibition by pre-incubation (30 min) with 10 µg of SARS-CoV-2 RBD (Figure 6D). Collectively, this finding suggests that SARS-CoV-2 spike proteins bind directly to full-length ACE2 through the RBD and thus abolish ACE2 activity.

Evaluation by debulking of SARS-CoV-2 in saliva by ddPCR

Several de-identified saliva samples collected from patients positive for SARS-CoV-2 were used to evaluate debulking of the viral particles by ACE2 or placebo gum using droplet digital PCR (ddPCR). Unlike the microbubble assay in which actual viral particles are measured, ddPCR amplifies and then quantifies the viral RNA, and therefore actual copies of viral RNA present in patients is not directly measured. While PCR amplification is used to increase sensitivity of saliva tests, it is not quantitative. Therefore, PCR amplification has not yet been used to predict the severity of COVID-19 disease. Despite these limitations with the nucleic acid testing approach, we observed some reduction with the placebo and significant reduction with ACE2 gum in COVID-19 saliva samples, almost to the lowest number of copies that could be reliably measured by ddPCR (Figure 7).

DISCUSSION

The oral cavity is an important portal of entry for SARS-CoV-2 virus and plays a particularly significant role in the transmission of infection or continued re-infection. The heterogeneity of the oral mucosa at a cellular level and presence of several ubiquitous receptors including ACE2 and GM1 facilitate entry of oral pathogens.[47,49–51] Saliva plays a vital role in transmission of infection among critically ill patients and can also compromise oral tissues.[52] Reducing the viral load in saliva should limit the risk of transmission from a potential carrier[53–55] and may help reduce the severity of COVID-19 disease by minimizing re-infection because salivary glands constitute the primary site of SARS-CoV-2 replication. Therefore, we explore the ability of CTB-ACE2 chewing gum to trap SARS-CoV-2 to debulk virus from saliva in pre-clinical studies that provide a foundation of clinical testing designed to reduce oral viral load and transmission.

ACE2 is an integral part of the renin-angiotensin system (RAS), and cleaves angiotensin II (Ang II), which causes vasoconstriction, inflammation, hypercoagulation, and fibrosis[19] to produce the anti-inflammatory, cytoprotective angiotensin 1–7 (Ang 1–7) peptide. Human ACE2 exists in both the soluble (sACE2) and membrane-associated ACE2 (mACE2) forms, the latter being the most predominant form.[20,21,56] Infusion could supplement the lost sACE2 and help balance RAS by prevention of downregulation in COVID-19 patients.[22] In pulmonary hypertension (PH) disease with disease symptoms

Please cite this article in press as: Daniell et al., Debulking SARS-CoV-2 in saliva using angiotensin converting enzyme 2 in chewing gum to decrease oral virus transmission and infection, Molecular Therapy (2021), https://doi.org/10.1016/j.ymthe.2021.11.008

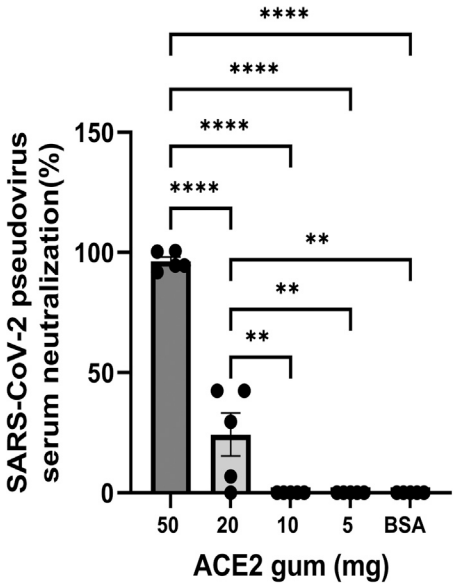

Figure 4. ACE2 gum inhibits SARS-CoV-2 pseudoviral infectivity *in vitro*

SARS-CoV-2 spike glycoprotein pseudotyped viruses expressing luciferase were incubated with ACE2 gum at the indicated concentration for 90 min at room temperature. Following centrifugation, virus-containing supernatant was incubated with ACE2-expressing CHO cells for 72 h, and viral infectivity was measured via luciferase. Data are representative of three independent experiments with N = 2–3 samples. Bars represent the condition mean, symbols represent the average of duplicate or triplicate assays, and error bars represent the SEM. **p < 0.01, ***p < 0.001, ****p < 0.0001 by Kruskal-Wallis ANOVA.

similar to those of COVID-19, oral ACE2 attenuates PH with a decrease in right ventricular (RV) hypertrophy, RV systolic pressure, total pulmonary resistance, and pulmonary artery remodeling.[43,57] In contrast to injected truncated (transmembrane deleted) sACE2,[22] full-length oral CTB-ACE2 accumulates in the lungs at 10-fold higher concentrations than in the plasma upon oral delivery of bioencapsulated plant cells,[43,44] offering yet another approach to treat COVID-19 patients.

Utilizing the concepts described above, ACE2 chewing gum is investigated here to trap SARS-CoV-2 to debulk virus and reduce oral transmission. While entry of SARS-CoV-2 into human cells through the ACE2 receptor has been widely reported,[34] the requirement for GM1 co-receptor or direct binding of the spike protein to soluble ACE2 has received less attention. In fact, SARS-CoV-2 has greater binding affinity to monomeric soluble ACE2 than other known coronaviruses.[21] CTB-ACE2 saturation of both ACE2/GM1 receptors located in close proximity[35,36] enabled virus neutralization studies in Vero cells using VSV or lentivirus engineered to express spike proteins or to prevent entry into human oral epithelial cells. Therefore, sACE2 could compete for the receptor-binding site with SARS-CoV-2 and act as "decoy" and also directly bind to SARS-CoV-2 spike protein, preventing entry into human cells.[44,56] Lentivirus particles expressing spike were used to accurately mimic entry of SARS-CoV-2 into ACE2-expressing cells (ACE2 293) by measuring luciferase activity. This system clearly demonstrated that ACE2 gum blocks infection of the spike-pseudotyped lentivirus particles in a dose-dependent manner. Significantly, infection of the spike-pseudotyped lentivirus particles was blocked by about 95% with 50 mg of ACE2 gum. Similarly, recombinant CTB-ACE2 and increasing concentrations of ACE2 gum powder effectively inhibited entry of VSV expressing S protein, compared with controls, when measured using red fluorescence.[42] Incubation of COVID samples with ACE2 gum significantly reduced the microbubble counts at femtomolar concentration,[40,41] confirming that ACE2 gum dramatically decreased the amount of nucleocapsid antigens. Unlike the microbubble assay where actual viral particles are measured, ddPCR quantifies viral RNA, which may not necessarily be associated with virions and has been shown to persist after clearance of active infection.[58,59] Despite these limitations with the nucleic acid testing approach, we observed significant reduction with ACE2 gum in COVID-19 saliva samples, almost to the lowest number of copies that could be reliably measured by ddPCR.

We observed that placebo gum without ACE2 had some antiviral activity, depending on viral particle density. In previous studies, *in silico* screening of 48 sugar alcohol compounds sorbitol, mannitol, and galactitol showed maximum binding to viral proteins, especially Ebola VP40.[60] ACE2 chewing gum contains maltitol (20.4%) and 13% each of sorbitol and xylitol, similar to commercial chewing gums, and could explain this placebo effect. In addition to demonstrating debulking of SARS-CoV-2 using several evaluation criteria, in this study we demonstrate the feasibility of clinical-grade plant biomass that can be prepared to meet FDA criteria. We followed guidelines based on FDA approval of Ara h proteins expressed in peanut cells for treatment of peanut allergy by oral delivery of plant cells.[61,62] Importantly, total aerobic microbial count and total yeast and mold counts in batches used for preparation of ACE chewing gum were within acceptance criteria established by the FDA for a non-aqueous drug product being delivered by the oral route. Furthermore, moisture content was less than 10%, as reported in the peanut allergy clinical trials (NCT02635776). Indeed, oral delivery of protein drugs bioencapsulated in plant cells reduces production and delivery costs by elimination of prohibitively expensive fermentation, purification, and cold chain maintenance for transportation/storage and sterile injections.[44,45,63] Most recently, the Daniell lab also developed the chewing gum expressing lipase, dextranase, and mutanase to disrupt dental biofilm and kill pathogenic bacteria and fungi.[64] In chewing gum tablets formulated with freeze-dried plant cells, GFP was stable up to 3 years at ambient temperature and was efficiently released in a time-dependent manner in a mechanical chewing simulator device, suggesting feasibility of the therapeutic gum for topical drug delivery. In this study, 90% of protein release from the chewing gum was observed using a chewing simulator machine (Pickering Laboratories) and artificial saliva.[64] We do not anticipate significant changes between *in vitro* experiments and oral cavity virus debulking experiments because complete debulking of virus in saliva was achieved with 50 mg of gum powder in the *in vitro* experiments, but each chewing gum weighs 2 g. A load range of −1.5 to −500 N for intervals of 1,

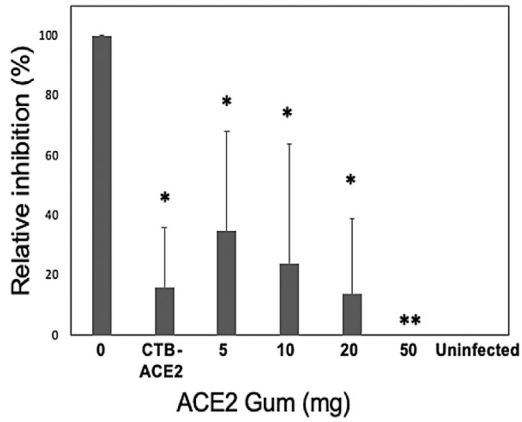

Figure 5. Impact of ACE2 on entry of VSV-spike particles

Relative inhibition of VSV-S particle entry after incubation with CTB-ACE2 or ACE2 gum powder was calculated to be statistically significant in all treatment groups, as compared with the untreated VSV-S control. The graph is representative of two replicates in two independent experiments (Student's t test, *$p < 0.05$, **$p < 0.01$).

5, 7, and 10 min and cycles of 55, 287, 364, and 591 simulates human chewing. However, a wide range of bite forces have been reported for adult humans. Values ranging from 1,300 to 285 N have been reported.[65,66] Varga and co-workers reported mean bite force values of 522 N for males and 465 N for females with normal occlusion.[67] Therefore, there may be differences in the release kinetics of ACE2, but a large dose of ACE2 in the chewing gum should compensate for differences in release kinetics in the oral cavity among patients. However, performing release experiments in the oral cavity requires FDA approval. IND has been filed, but conducting human clinical studies is beyond the scope of this article.

Saliva from COVID-19 patients show epithelial cells with ACE2 expression using single-cell RNA sequencing or transcriptomic studies, and the salivary viral burden correlates well with the severity of COVID-19, especially the loss of taste and smell,[12] but ACE2 activity has never been reported from saliva. Therefore, in this study, we evaluated ACE2 activity in healthy and COVID-19 saliva samples (Table S1). Healthy patients included five females (3 white/1 Asian/1 Caucasian) and five males (3 white/2 Asian), of the age group 25 through 69. All of them showed high ACE2 activity (93–446 mU/mg). Among COVID-19 patients, two are in their 40s (male, female—white/black), five in their 50s (4 females—2 white/2 black; 1 male—black), and three in their 60s (male/white). All COVID patients were tested positive, and PCR data are provided in Table S1. All COVID-19 saliva samples showed low or almost undetectable ACE2 activity (50% below zero and others 10–40 mU/mg). However, one patient was asymptomatic based on the patient chart and did not develop the COVID-19 disease, although PCR data showed the presence of SARS-CoV-2. Therefore, saliva ACE2 activity could serve as a biomarker to distinguish symptomatic from asymptomatic COVID-19 patients. The decrease in ACE2 activity observed in saliva could be due to downregulation of RAS47–48.[68,69] Alternatively or in addition, SARS-CoV-2 spike protein, which has high affinity to soluble ACE2, could bind directly and thus decrease ACE2 activity.[21] Indeed, this is strongly supported by our studies where RBD binds with much higher affinity than S1-S2 spike protein, fully inhibiting ACE2 activity.

While this study focuses on debulking SARS-CoV-2, the concept of trapping viral particles in the oral cavity using viral surface proteins in chewing gum to minimize re-infection or transmission could be applied to most other oral viruses including influenza, SARS, HPV, HSV, Epstein-Barr, Zika, and herpesvirus that complete their life cycle in the oral epithelium.[15] Flu influenza virus is one among the most transmitted seasonal viruses. Almost 40% of the flu virion surface is covered by two spike proteins, with 350 spikes of hemagglutinin (H subtype) and 70 spikes of neuraminidase (N subtype).[70] Influenza viruses bind to sialic acid human HA receptors and HA avian receptor can switch via several pathways, posing threat very similar to SARS-CoV-2 transition from bat to human host. New flu vaccines are developed for each seasonal flu owing to antigenically drifted variants.[71] Influenza virus transmission could also be decreased by debulking the virus with plant lectins in chewing gums, based on recent reports that the lectin FRIL is capable of neutralizing influenza or SARS-CoV-2 viruses at nanomolar concentrations.[72]

The oral cavity is an important portal of entry for viruses and plays an important role in transmission of infection. The oral cavity also contains several ubiquitous receptors including ACE2 and GM1 that facilitate entry of oral pathogens. Saliva plays a vital role in transmission of infection and offers great potential for diagnosis of metabolic and infectious diseases. Several SARS-CoV-2 variants that change clinical manifestations, transmissibility, morbidity, and mortality are identified on a regular basis.[73–77] Therefore, reducing the viral load using ACE2 chewing gum will not only help in mitigating the severity of COVID-19 variants but also limit the risk of transmission from a potential carrier.[53–55] While current chewing gum used the native full-length human ACE2 protein, future studies could explore engineered ACE proteins that have 170-fold higher affinity to SARS-CoV-2 spike protein to bind to evolving variants[23,24] and efficiently block infection or transmission.

In summary, this is the first report of use of a biomaterial to debulk SARS-CoV-2 in saliva. Transmission of SARS-CoV-2 is an urgent concern around the globe due to emerging variants, inadequate vaccination, and limitation of current containment methods. This report offers a novel and affordable concept to reduce SARS-CoV-2 re-infection through saliva and minimize oral aerosol transmission, and offers patients time to build immunity in countries where vaccines are not available or affordable. In particular, this is a novel approach to protect individuals at home and also healthcare workers from patients without masks during oral procedures and dental cleaning. There are no examples of FDA-approved antiviral biologic traps, making this a novel approach. In addition, we utilize virus quantitation without any nucleic acid amplification by using recently developed microbubble technology, which is capable of detecting viral surface protein signals. ACE2 activity is also quantified for the first

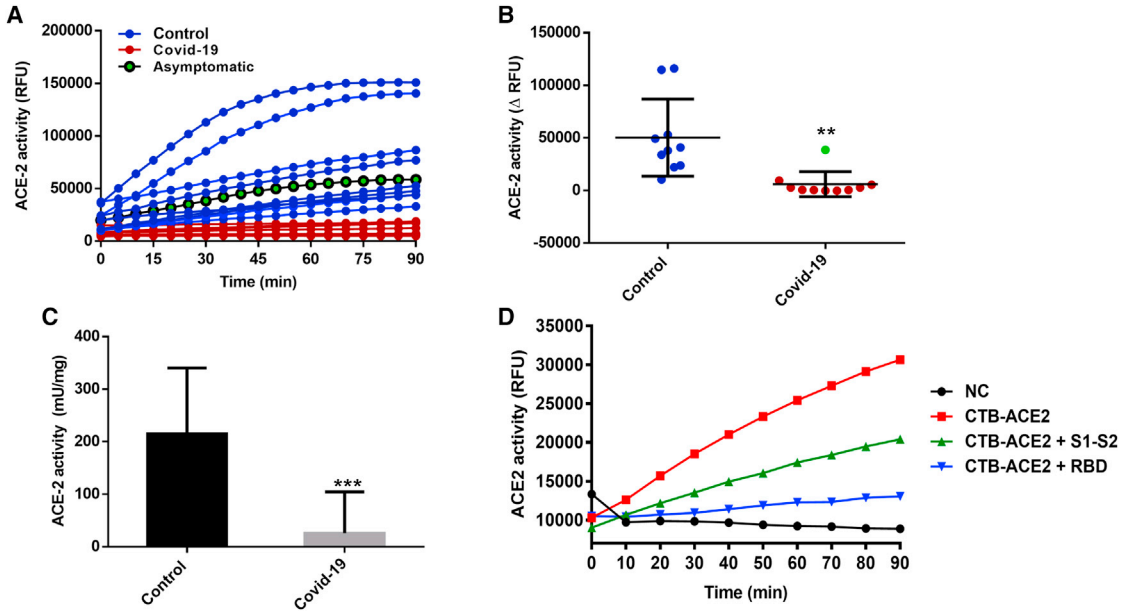

Figure 6. Kinetic reading of ACE2 in saliva- and plant-derived full-length ACE2

(A and B) ACE2 activity determined by cleavage of fluorogenic Mca-APK (Dnp) substrate in ten control and ten COVID (red) samples. ΔRFU was calculated by subtracting data of time point 0 min from data of time point 90 min. Data were analyzed using the Student's t test; **$p < 0.0019$. (C) ACE2 enzyme activity presented as enzyme units (mU/mg). Data were analyzed using the Student's t test; ***$p < 0.0008$. (D) Interaction of full-length CTB-ACE2 with or without recombinant SARS-CoV-2 spike proteins. ACE2 activity was measured using 20 μg of CTB-ACE2 protein extracts by cleavage of fluorogenic Mca-APK (Dnp) substrate in the presences and absence of 10 μg of spike proteins (SARS-CoV-2 RBD and SARS-CoV-2 S1-S2). NC, negative control (substrate and buffer only).

time in human saliva, with striking reductions demonstrated among COVID-19 patients. Demonstration that the viral spike protein binds avidly to soluble ACE2 provides a mechanism for *in vitro* saliva debulking with CTB-ACE2 in chewing gum. Direct correlation of ACE2 activity inhibition to SARS-CoV-2 infection, and ability to distinguish asymptomatic from symptomatic COVID-19 PCR-positive patients offers unique ability to identify a potential new biomarker. Recent reports show that the delta variant has >1,000-fold her viral load in saliva and, therefore, it is important to debulk SARS-CoV-2 in saliva.[3,4] While masks can prevent transmission to others, they do not protect re-infection of infected individuals. Therefore, chewing gum as a biomaterial offers novel and practical applications during the current pandemic.

MATERIALS AND METHODS

Saliva sample collection

After informed consent under protocol #823392 approved by the UPenn IRB, saliva and swabs of the nasopharynx and oropharynx were obtained from hospitalized patients with confirmed SARS-CoV-2 infection. Saliva was produced by patients spontaneously, and oropharyngeal and nasopharyngeal samples were collected with flocked nylon swabs (Copan Diagnostics) and eluted together in 2 mL of viral transport medium. Saliva from healthy volunteers (confirmed SARS-CoV-2 negative) was collected following informed consent under protocol #842613 approved by the UPenn IRB. Specimens were stored at −80°C until use.

Plant growth at Fraunhofer USA, biomass harvest, and lyophilization

The hydroponic growth system at Fraunhofer USA includes multi-level growth racks illuminated to grow the transplastomic lettuce expressing CTB-ACE2. Growth trays contained rockwool, a lightweight hydroponic substrate that is manufactured by spinning molten basaltic rock into fibers, as the supporting substrate (Grodan, the Netherlands). Rockwool is designed to hold approximately 80% nutrient solution, with approximately 15% air space and 5% fibers, drains freely, and encourages rapid uptake of nutrient solution by plant root systems. The final nutrient solution for hydroponic growth comprised Peters Professional general purpose fertilizer at 200 parts per million nitrogen with a 20:10:20 ratio of nitrogen, phosphate, and potash (potassium oxide) (ICL Fertilizers, OH), and YaraLiva Calcinit (nitric acid, ammonium calcium salt) (Yara North America) at 102 parts per million calcium. Nutrient concentrates were supplied via Dosatrons at a 1:100 injection ratio with potable water. Seedlings were spaced at 8.5 inches on a diagonal grid on the rockwool surface. Plants were exposed to LED lighting (Fluence SPYDRx) at an average of 368 μmol/m^2·S on a 16-h day/8-h night photoperiod under conditions of temperature (24°C ± 2°C day/20°C ± 2°C night) and humidity (60% ± 10%) in a growth room. Air flow across the plants was approximately 1.2 m/s.

At Fraunhofer, the transplastomic lettuce was repeatedly harvested from plants on days 58, 90, 107, and 120 post seeding, typically at

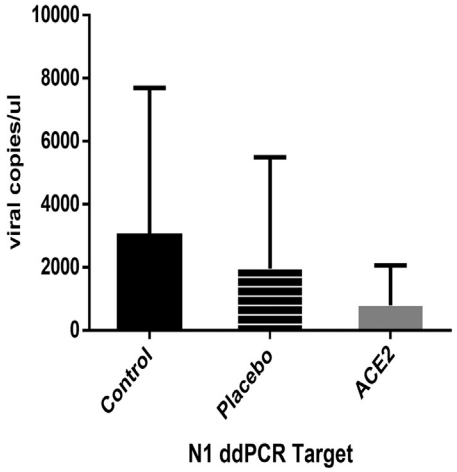

Figure 7. Reduction of COVID-19 copies detected by ddPCR in chewing gum incubation

COVID-19-positive saliva samples were incubated with ACE2 powder gum. N1 target is specific to SARS-CoV-2 and is reduced by ACE2 chewing gum. Standard deviation reflects extensive variation of N1 copy number among saliva samples examined.

approximately 9 (8–11) hours into the day portion of the photoperiod, while the AeroFarms grown plants were harvested 79 and 100 days post seeding. The leaves of lettuce plants were cut at the base of the petiole by operators wearing laboratory gloves, leaving the upper leaves intact on each plant, and the fresh weight of biomass harvested was recorded. Leaves were rinsed in USP purified water, washed for approximately 5 min in a 200 parts per million chlorine solution prepared using food-grade calcium hypochlorite, and rinsed three consecutive times in USP purified water, with final chlorine levels measured using chlorine sanitizer test strips to ensure levels were less than 4 parts per million. Excess water was then removed from leaf surfaces using a food-grade centrifugal lettuce drier before being transferred to polyvinyl zip-top bags. Bags were frozen on dry ice and then progressed to storage at $\leq -60°C$ to $-80°C$. Frozen lettuce leaves expressing CTB-ACE2 fusion proteins were freeze-dried in a lyophilizer (Ultra50; SP Scientific, Stone Ridge, NY).

Shelves were pre-cooled to $-40°C$ and each of the 15 shelves loaded with frozen leaves that had been briefly pounded with a mallet and from which remaining sizable pieces of petiole had been removed (typically loading approximately 0.5 kg per shelf), with lyophilizer thermocouple probes placed in the middle of plant materials in every other tray to monitor product temperature. The lyophilization cycle was optimized to reduce the duration of the cycle time in order to maximize throughput, while achieving a sufficiently low moisture content of at least $\leq 10\%$ and preferably $\leq 5\%$ for further processing, with a preferred cycle comprising the following sequence. Lyophilization started with a freezing phase, holding plant materials at $-40°C$ for 180 min at a vacuum of 300 mTorr. This was followed by a drying phase that comprised the following stages: holding at $-40°C$ for 15 min at a vacuum of 300 mTorr, then ramping to $-5°C$ over a period of 350 min followed by holding at $-5°C$ for 180 min at a vacuum of 300 mTorr, then ramping to 25°C over a period of 300 min followed by holding at 25°C for at least 1,000 min at a vacuum of 300 mTorr, and finally holding at 25°C for a further 500 min at a vacuum of 300 mTorr. A PVG/CM of 43 mTorr needed to be reached before progression to the final holding step in the above cycle. After the cycle ended, plant materials were unloaded, packed, weighed, and assessed for moisture content. The lyophilizer was thoroughly cleaned and disinfected after each use and records collected on cycle parameters. If not proceeding directly to milling, the materials were placed into zip-top bags and then into light-tight storage bags. The freeze-dried materials were stored in dark cabinets at room temperature in a storage room. The lyophilized leaves were ground in a grinder (BioMix-700g) at single speed once for 3 s (optimized for minimal disrupted cells). The milled powder was poured over a 25-mesh (0.71 mm) hand sieve into the final sterile container for closure. Any material that did not pass through the sieve was discarded. The materials were stored in sterile containers (FDA approved) inside a steel cabinet for dark, room-temperature storage and assessed for bioburden.

Moisture content

Moisture content was determined by Karl Fischer titration, whereby available water reacts with iodine and sulfur dioxide to form sulfur trioxide and hydrogen iodide. In brief, samples were weighed, and sample vials capped and placed in a Metrohm 850 KF Thermoprep and heated to 150°C. Vaporized water from samples was pumped into a Metrohm 851 Titrando at a rate of 50 mL/min. Percentage of moisture was calculated from sample weight and reaction output, with Hydranal water standard (Honeywell) as a reference control. A recent model of freeze dryer (Virtis Ultra 50) has new gadgets to evaluate and monitor moisture content, which were not available in previous versions.

Bioburden

Following harvest of biomass, leaves were washed in a 200 parts per million chlorine solution with triple rinse in USP purified water. Excess water was then removed from leaves and the tissue frozen and stored. The tissue was then freeze-dried in a lyophilizer (Ultra50; SP Scientific), assessed for moisture content, ground, and sieved and again assessed for moisture content and for bioburden. Bioburden was evaluated according to USP <61> (microbiological examination of nonsterile products: microbial enumeration tests) and USP <62> (microbiological examination of nonsterile products: tests for specified microorganisms). Samples were assessed for aerobic microbial and fungal loads by plating serial dilutions in duplicate on each of trypticase soy agar and Sabouraud dextrose agar, respectively, and incubating for 3–5 days at 30°C–35°C or 5–7 days at 20°C–25°C, respectively. For oral delivery, acceptance criteria were set according to USP <1111> (microbial examination of nonsterile products: acceptance criteria for pharmaceutical preparations and substances for pharmaceutical use) at $\leq 2 \times 10^3$ CFU/g for total aerobic microbial count and $\leq 2 \times 10^2$ CFU/g for total yeast and mold count.

Total protein extraction and quantification of ACE2

CTB-ACE2 expression was examined by western blots as described previously,[39] with suitable modifications. Ten milligrams of lyophilized plant powder was extracted with 500 μL of protein extraction buffer containing 100 mM NaCl, 10 mM EDTA (pH 8), 200 mM Tris (pH 8), 100 mM dithiothreitol, 1× protease inhibitor cocktail, 2 mM phenylmethylsulfonyl fluoride, and 10 mM β-mercaptoethanol. The homogenates were incubated for 1 h while vortexing at 4°C. This was followed by sonication of samples at 80% amplitude for 10 s on and 15 s off (6×) using a sonicator 3000 (Misonix, Farmingdale, NY). Bradford assay was used to quantify total protein content (Bio-Rad Laboratories, Hercules, CA). After adding 1× Laemmli buffer, homogenized proteins were heated at 70°C for 15 min on a hot plate and run on 10% SDS-PAGE. For each Fraunhofer and AeroFarms sample, two different concentrations of total protein were loaded on gels, Plant materials across different harvests, 58- to 120-day-old plants grown at Fraunhofer were compared with 79- to 107-day-old plants grown at AeroFarms.

For all immunoblot analyses, anti-CTB antibody (1:10,000) (Gen Way Biotech, San Diego, CA), goat antirabbit IgG-HRP secondary antibody (1:4,000) (Southern Biotechnology, Birmingham, AL), and the Precision Plus protein standard (Bio-Rad Laboratories) were used. The West Pico Chemiluminescent substrate (Thermo Fisher Scientific, Waltham, MA) was used to detect ACE2 proteins on iBright Western Blot Imaging Systems (Thermo Fisher Scientific). Different concentrations of CTB standard were used to quantify ACE2 protein using iBright Analysis Software (Thermo Fisher Scientific). Total protein content of plant samples was quantified in three technical replicates performed in eight independent experiments.

ACE2 enzyme activity assay in plant extract and saliva

ACE2 activity assay was performed using saliva of SARS-CoV-19 affected and healthy people. Saliva samples were prepared at 1:5 dilution. Seventy-five microliters of this prepared sample was added to a black 96-well microtiter plate containing 25 μL of ACE2 buffer (50 μmol/L $ZnCl_2$, 75 mmol/L Tris-HCl [pH 7.5], and 1 mol/L NaCl), and 20 μmol/L ACE2-specific fluorogenic peptide substrate VI Mca-APK(Dnp) (R&D Systems, Minneapolis, MN). The enzymatic activity was recorded for 90 min at 5-min intervals at 28°C with optic position top and gain extended; with excitation at 340 nm and emission at 405 nm. The relative fluorescence unit at each time point was plotted. ΔRFU was calculated by subtracting data of time point 0 min from the data of time point 90 min. Total soluble protein in the remaining saliva sample was determined by Bradford assay using standard Daniell lab protocol. The final ACE2 enzyme activity was calculated as pmol/min/mg (mU/mg) = Δpmol/90 min/mg total protein.

Microbubble SARS-CoV-2 antigen assay

Patient samples (150 μL) were added to each powder tube and vortexed. Tubes were then incubated at 4°C for 1 h while rotating. Following incubation, tubes were vortexed again, then spun at 14,000 rpm for 20 min at 4°C. Tubes were recovered and 120 μL of supernatant was first mixed with virus lysis buffer of 10% Tween 20 (100×, 1.2 μL) and 100× protease inhibitor cocktail (1.2 μL) and incubated at room temperature for 30 min. The lysed sample was then tested with the Microbubble SARS-CoV-2 Antigen Assay.[40,41] In brief, sample solutions (100 μL) were incubated with suspensions of 500,000 capture antibody functionalized magnetic beads, on a roller (12 rpm) at room temperature for 30 min. The beads were then separated using magnets and washed three times with PBS buffer (pH 7.4) containing 0.01% Tween 20, then resuspended in 100 μL of 250 ng/mL biotinylated detection antibody in PBS containing 1% BSA, on a roller (12 rpm) at room temperature for 30 min. The beads were then separated using magnets and washed three times with PBS buffer (pH 7.4) containing 0.01% Tween 20 and then resuspended in 100 μL of 1 μg/mL NeutrAvidin functionalized Pt nanoparticles in PBS containing 1% BSA, on a roller (12 rpm) at room temperature for 30 min. The beads were then separated using magnets and washed three times with PBS buffer (pH 7.4) containing 0.01% Tween 20 and resuspended in 100 μL of 30% H_2O_2. The magnetic bead slurries were then added into the chambers of the microbubbling microchips. The microbubbling microchips were placed on a neodymium disk magnet for 1 min to pull down the beads to the bottom of the microchips. Microbubbles on the microbubbling microchips were imaged using an iPhone 11 or an iPad with the uHandy mobile phone microscope (9×, 5 mm focusing length; Aidmics Biotechnology, Taipei, Taiwan).

Neutralization assay with SARS-CoV-2 spike-pseudotyped lentiviral particles

SARS-CoV-2 pseudovirus was produced using HEK293T cells transfected with a 1:1 ratio of IgE-SARS-CoV-2 S plasmid (Genscript) and pNL4-3.Luc.R-E^- plasmid (NIH AIDS reagent) using Gene Jammer (Agilent) as transfection reagent. Forty-eight hours post transfection, transfection supernatant was collected, enriched with fetal bovine serum (FBS) to 12% final volume, and stored at −80°C. SARS-Cov-2 pseudovirus neutralization assay was set up using D10 medium (DMEM supplemented with 10% FBS and 1× penicillin-streptomycin) in a 96-well format using huCHOAce2 cells (Creative Biolabs, catalog no. VCeL-Wyb019). For neutralization assay, 10,000 CHO-ACE2 cells were plated in 96-well plates and rested overnight at 37°C and 5% CO_2 for 24 h. CTB-ACE2 cells at specific weights were incubated with a fixed amount of SARS-Cov-2 pseudovirus for 90 min at room temperature in complete medium. After centrifugation at 15,005 rpm for 10 min, the supernatant of this mix was added to huCHOAce2 cells and allowed to incubate in a standard incubator (37% humidity, 5% CO_2) for 72 h. After 72 h, cells were lysed using the Britelite Plus luminescence reporter gene assay system (PerkinElmer, catalog no. 6066769), and relative light units were measured using a BioTek plate reader. Percent neutralization was calculated using GraphPad Prism 8.

VSV-S-pseudotyped neutralization assay

VSV-S pseudotype particles were generated using a VSV platform described previously.[42] In brief, pseudotyped VSV virions that incorporate the SARS-CoV-2 spike protein into their envelopes were produced by transfection of HEK293T cells with pCG1 SARS-CoV-2 S delta18 expression plasmid encoding a codon optimized SARS-

CoV-2 S gene with an 18-residue truncation in the cytoplasmic tail (kindly provided by Paul Bates and Stefan Pohlmann). At 30 h post transfection, the SARS-CoV-2 spike-expressing cells were transduced for 4 h with VSVΔG-RFP pseudotypes. The viral inoculum was removed, and the cells were washed twice with 1× PBS to remove unbound virus. At 28 h post transduction, the medium containing the VSV-S pseudotypes was harvested and clarified by centrifugation twice at 4,000 rpm for 15 min. VSV-S pseudotypes were aliquoted and stored at −80°C until use in ACE2 neutralization studies.

Vero E6 cells were seeded at 1×10^4 cells per well in a 96-well plate and incubated overnight at 37°C. One hundred microliters of VSV-S pseudotype particles (~1.2×10^4 red fluorescent units) in medium were mixed with 250 ng of CTB-ACE2 or 5 mg, 10 mg, 20 mg, or 50 mg ACE2 gum powder and rotated end over end for 30 min at 4°C. Samples were centrifuged at 14,800 rpm for 20 min at 4°C to pellet the gum powder, and the supernatant was added to Vero cells for 1 h at 37°C, swirling every 15 min. Virus inoculum was removed, and the cells were washed twice with 1× PBS to remove unbound viral particles. At 24 h post transduction, RFP expression was visualized and quantified on a fluorescent microscope. RFP expression in each condition was measured in two technical replicates performed in two independent experiments. Inhibition of VSV-S entry was calculated relative to the untreated VSV-S control, and statistical significance was analyzed by Student's t test.

ddPCR assay

Fifteen saliva specimens from COVID-19 patients were collected by UPenn under an IRB-approved protocol. Saliva (140 μL) was mixed and incubated with 100 mg of ACE2 or placebo gum powder for 1 h at room temperature while rotating, then spun at 14,000 rpm for 20 min. Manufacturer's instructions were followed while using the QIAamp viral RNA mini kit (Qiagen), and total RNA was extracted from the supernatant. ddPCR was performed in duplicates via the COVID-19 digital PCR detection kit (Bio-Rad). The QX200 Droplet Digital PCR System using Supermix probe (Bio-Rad) was used following the manufacturer's instructions. The kit allows detection of the regions of nucleocapside N1, N2 gene, and Rnase P gene positive reference gene. QX200 droplet generator (Bio-Rad) converted 22 μL of each reaction mix to droplets. Soon after transferring and sealing the droplet partitioned specimens to a 96-well plate, they were cycled in a T100 Thermal Cycler (Bio-Rad) following the protocol: DNA polymerase activation at 95°C for 10 min, denaturation at 94°C for 30s and final step of annealing at 60°C for 1 min, followed by 4-degree infinite hold. Using the QX200 reader (Bio-Rad) the cycled plate was read in the HEX and FAM channels. QuantaSoft analysis Pro 1.0.596 software (Bio-Rad) was used for data interpretation.

SUPPLEMENTAL INFORMATION

Supplemental information can be found online at https://doi.org/10.1016/j.ymthe.2021.11.008.

ACKNOWLEDGMENTS

The authors thank Dr. Csanad Gurdon for growth of plants at AeroFarms and Dr. Imran Khan for help in harvesting. The authors are grateful to Ms. Leslie Mather for offering her expertise in optimizing Ultra50 lyophilization cycle optimization and Ms. Abigail Mateson for exceptional help in setting up Ultra50. Moisture content and bioburden assays were conducted by Mr. Kevin Stecca and Ms. Niketa Langalia, respectively, at Fraunhofer USA. The authors thank Mr. Amir Schinnar for designing the greenhouse and sterile growth room facilities, Laura Sprague for daily project management, and Robert Muraglia, Roseann Wallin, and Jason Nestor for grants management. Funding: Research in the Daniell laboratory is supported by funding from NIH grants R01 HL 107904, R01 HL 109442, and R01 HL 133191. Commonwealth of Pennsylvania, Department of Community and Economic Development grant to H.D. on "COVID-19 Pennsylvania Discoveries: Responding to SARS-CoV-2 Through Innovation & Commercialization" funded the purchase of freeze dryers, toxicology studies on ACE2 produced at Fraunhofer USA/AeroFarms, and production of the chewing gum. Saliva sample collection in the Collman lab is supported by R33-HL137063. Research in the Harty laboratory is supported by funding from a University of Pennsylvania School of Veterinary Medicine COVID-19 Pilot Award, a Mercatus Center award, and NIH T32 grant AI070077 to A.S.-M. SARS-CoV-2 research in the Wang laboratory is supported by funding from the Penn Center for Precision Medicine, Penn Health-Tech, Penn Center for Innovation and Precision Dentistry, and NIH RADx program.

AUTHOR CONTRIBUTIONS

H.D. conceived this project, designed experiments, identified collaborators, and coordinated projects with different groups or institutions, interpreted data, and wrote/edited several versions of the manuscript. S.K.N. quantified CTB-ACE2 in chewing gum and performed ACE2 activity assays in saliva samples, and interpreted data. S.K.N., H.D., S.J.S., N.E., and SP Scientific experts optimized the recipe for the lyophilization cycles in Ultra50. N.E. freeze-dried plants grown at AeroFarms, and along with G.W., N.S., and P.K.G. quantified ACE2. Md.R.I. performed ACE2 assay in plant extract. At Fraunhofer USA, S.J.S. designed the growth conditions and contributed to the manuscript, R.M.-L. and B.J.G. contributed to the design of the growth process and optimization of the leaf washing protocol, and P.K. contributed to the design of the growth and lyophilization process. S.N.C. amd M.M. designed and performed ddPCR studies to evaluate SARS-CoV-2 copy number. M.M. seeded ACE2 plants and assisted with biomass growth, harvesting, processing, and lyophilization. J.G.-W. and R.G.C. contributed saliva samples. E.N.G., A.R.A., M.N., R.R., and D.B.W. performed and interpreted lentivirus spike neutralization assays. A.S.-M. and R.N.H. performed and interpreted VSV-spike pseudotype entry assays. P.W. and S.F. contributed nasopharyngeal swab samples, and performed and interpreted the microbubbling SARS-CoV-2 antigen assay. K.B.M. participated in discussions and edited the manuscript.

DECLARATION OF INTERESTS

All authors declare no competing interests except the corresponding author (H.D.), who is a patentee in this field but has no specific financial conflict of interest to disclose.

REFERENCES

1. Allen, J.G., and Ibrahim, A.M. (2021). Indoor air changes and potential implications for SARS-CoV-2 transmission. JAMA *325*, 2112–2113.
2. Stadnytskyi, V., Bax, C.E., Bax, A., and Anfinrud, P. (2020). The airborne lifetime of small speech droplets and their potential importance in SARS-CoV-2 transmission. Proc. Natl. Acad. Sci. U S A *117*, 11875–11877.
3. Bolze, A., Luo, S., White, S., Cirulli, E.T., Wyman, D., Dei Rossi, A., Machado, H., Cassens, T., Jacobs, S., Schiabor Barrett, K.M., et al. (2021). SARS-CoV-2 variant delta rapidly displaced variant alpha in the United States and led to higher viral loads. medRxiv. https://doi.org/10.1101/2021.06.20.21259195.
4. Li, B., Deng, A., Li, K., Hu, Y., Li, Z., Xiong, Q., Liu, Z., Guo, Q., Zou, L., Zhang, H., et al. (2021). Viral infection and transmission in a large, well-traced outbreak caused by the SARS-CoV-2 Delta variant. medRxiv. https://doi.org/10.1101/2021.07.07.21260122.
5. Volz, E., Hill, V., McCrone, J.T., Price, A., Jorgensen, D., O'Toole, A., Southgate, J., Johnson, R., Jackson, B., Nascimento, F.F., et al. (2021). Evaluating the effects of SARS-CoV-2 spike mutation D614G on transmissibility and pathogenicity. Cell *184*, 64–75.e11.
6. Wibmer, C.K. (2021). SARS-CoV-2 501Y.V2 escapes neutralization by South African COVID-19 donor plasma. bioRxiv. https://doi.org/10.1101/2021.01.18.427166.
7. Korber, B., Fischer, W.M., Gnanakaran, S., Yoon, H., Theiler, J., Abfalterer, W., Hengartner, N., Giorgi, E.E., Bhattacharya, T., Foley, B., et al. (2020). Tracking changes in SARS-CoV-2 spike: evidence that D614G increases infectivity of the COVID-19 virus. Cell *182*, 812–827.e19.
8. Lythgoe, K.A., Hall, M., Ferretti, L., de Cesare, M., MacIntyre-Cockett, G., Trebes, A., Andersson, M., Otecko, N., Wise, E.L., Moore, N., et al. (2021). SARS-CoV-2 within-host diversity and transmission. Science *372*. https://doi.org/10.1126/science.abg0821.
9. Li, Y., Ren, B., Peng, X., Hu, T., Li, J., Gong, T., Tang, B., Xu, X., and Zhou, X. (2020). Saliva is a non-negligible factor in the spread of COVID-19. Mol. Oral Microbiol. *35*, 141–145.
10. Liu, W.J., Xiao, H., Dai, L., Liu, D., Chen, J., Qi, X., Bi, Y., Shi, Y., Gao, G.F., and Liu, Y. (2021). Avian influenza A (H7N9) virus: from low pathogenic to highly pathogenic. Front. Med. https://doi.org/10.1007/s11684-020-0814-5.
11. Paules, C., and Subbarao, K. (2017). Influenza. Lancet *390*, 697–708.
12. Jang, Y.H., and Seong, B.L. (2019). The quest for a truly universal influenza vaccine. Front. Cell. Infect. Microbiol. *9*. https://doi.org/10.3389/fcimb.2019.00344.
13. Wu, Y., Wu, Y., Tefsen, B., Shi, Y., and Gao, G.F. (2014). Bat-derived influenza-like viruses H17N10 and H18N11. Trends Microbiol. *22*, 183–191.
14. Atyeo, N., Rodriguez, M.D., Papp, B., and Toth, Z. (2021). Clinical manifestations and epigenetic regulation of oral herpesvirus infections. Viruses *13*, 681.
15. Tewari, P., Banka, P., Kernan, N., Reynolds, S., White, C., Pilkington, L., O'Toole, S., Sharp, L., D'Arcy, T., Murphy, C., et al. (2021). Prevalence and concordance of oral HPV infections with cervical HPV infections in women referred to colposcopy with abnormal cytology. J. Oral Pathol. Med. https://doi.org/10.1111/jop.13172.
16. Wölfel, R., Corman, V.M., Guggemos, W., Seilmaier, M., Zange, S., Müller, M.A., Niemeyer, D., Jones, T.C., Vollmar, P., Rothe, C., et al. (2020). Virological assessment of hospitalized patients with COVID-2019. Nature *581*, 465–469.
17. Chan, J.F.W., Yip, C.C.Y., To, K.K.W., Tang, T.H.C., Wong, S.C.Y., Leung, K.H., Fung, A.Y.F., Ng, A.C.K., Zou, Z., Tsoi, H.W., et al. (2020). Improved molecular diagnosis of COVID-19 by the novel, highly sensitive and specific COVID-19-RdRp/Hel real-time reverse transcription-PCR assay validated *in vitro* and with clinical specimens. J. Clin. Microbiol. *58*, 10–20.
18. Huang, N., Pérez, P., Kato, T., Mikami, Y., Okuda, K., Gilmore, R.C., Conde, C.D., Gasmi, B., Stein, S., Beach, M., et al. (2021). SARS-CoV-2 infection of the oral cavity and saliva. Nat. Med. *27*, 892–903.
19. Gheblawi, M., Wang, K., Viveiros, A., Nguyen, Q., Zhong, J.C., Turner, A.J., Raizada, M.K., Grant, M.B., and Oudit, G.Y. (2020). Angiotensin-converting enzyme 2: SARS-CoV-2 receptor and regulator of the renin-angiotensin system: celebrating the 20th anniversary of the discovery of ACE2. Circ. Res. *126*, 1456–1474.
20. Rahman, M.M., Hasan, M., and Ahmed, A. (2021). Potential detrimental role of soluble ACE2 in severe COVID-19 comorbid patients. Rev. Med. Virol. https://doi.org/10.1002/rmv.2213.
21. Anand, S.P., Chen, Y., Prévost, J., Gasser, R., Beaudoin-Bussières, G., Abrams, C.F., Pazgier, M., and Finzi, A. (2020). Interaction of human ACE2 to membrane-bound SARS-CoV-1 and SARS-CoV-2 S glycoproteins. Viruses *12*. https://doi.org/10.3390/v12101104.
22. Zoufaly, A., Poglitsch, M., Aberle, J.H., Hoepler, W., Seitz, T., Traugott, M., Grieb, A., Pawelka, E., Laferl, H., Wenisch, C., et al. (2020). Human recombinant soluble ACE2 in severe COVID-19. Lancet Respir. Med. *8*, 1154–1158.
23. Glasgow, A., Glasgow, J., Limonta, D., Solomon, P., Lui, I., Zhang, Y., Nix, M.A., Rettko, N.J., Zha, S., Yamin, R., et al. (2020). Engineered ACE2 receptor traps potently neutralize SARS-CoV-2. Proc. Natl. Acad. Sci. U S A *117*, 28046–28055.
24. Bracken, C.J., Lim, S.A., Solomon, P., Rettko, N.J., Nguyen, D.P., Zha, B.S., Schaefer, K., Byrnes, J.R., Zhou, J., Lui, I., et al. (2021). Bi-paratopic and multivalent VH domains block ACE2 binding and neutralize SARS-CoV-2. Nat. Chem. Biol. *17*, 113–121.
25. Strauch, E.M., Bernard, S.M., La, D., Bohn, A.J., Lee, P.S., Anderson, C.E., Nieusma, T., Holstein, C.A., Garcia, N.K., Hooper, K.A., et al. (2017). Computational design of trimeric influenza-neutralizing proteins targeting the hemagglutinin receptor binding site. Nat. Biotechnol. *35*, 667–671.
26. Chen, T., and Hudnall, S.D. (2006). Anatomical mapping of human herpesvirus reservoirs of infection. Mod. Pathol. *19*, 726–737.
27. Laane, C.J., Murr, A.H., Mhatre, A.N., Jones, K.D., and Lalwani, A.K. (2002). Role of Epstein-Barr virus and cytomegalovirus in the etiology of benign parotid tumors. Head Neck *24*, 443–450.
28. Ferreiro, M., Dios, P., and Scully, C. (2005). Transmission of hepatitis C virus by saliva? Oral Dis. *11*, 230–235.
29. Musso, D., Roche, C., Nhan, T.X., Robin, E., Teissier, A., and Cao-Lormeau, V.M. (2015). Detection of Zika virus in saliva. J. Clin. Virol. *68*, 53–55.
30. Liu, Y., Gayle, A.A., Wilder-Smith, A., and Rocklöv, J. (2020). The reproductive number of COVID-19 is higher compared to SARS coronavirus. J. Trav. Med. *27*. https://doi.org/10.1093/jtm/taaa021.
31. del Rio, C., Malani, P.N., and Omer, S.B. (2021). Confronting the delta variant of SARS-CoV-2, summer 2021. JAMA, E1–E2. https://doi.org/10.1001/jama.2021.14811.
32. Scientific Advisory Group for Emergencies. SPI-M-O: Consensus Statement on COVID-19, 30 June 2021. https://www.gov.uk/government/publications/spi-m-o-consensus-statement-on-covid-19-30-june-2021.
33. To, K.K.W., Tsang, O.T.Y., Yip, C.C.Y., Chan, K.H., Wu, T.C., Chan, J.M.C., Leung, W.S., Chik, T.S.H., Choi, C.Y.C., Kandamby, D.H., et al. (2020). Consistent detection of 2019 novel coronavirus in saliva. Clin. Infect. Dis. *71*, 841–843.
34. Wrapp, D., Wang, N., Corbett, K.S., Goldsmith, J.A., Hsieh, C.L., Abiona, O., Graham, B.S., and McLellan, J.S. (2020). Cryo-EM structure of the 2019-nCoV spike in the prefusion conformation. Science *367*, 1261263.
35. Fantini, J., Chahinian, H., and Yahi, N. (2020). Synergistic antiviral effect of hydroxychloroquine and azithromycin in combination against SARS-CoV-2: what molecular dynamics studies of virus-host interactions reveal. Int. J. Antimicrob. Agents *56*. https://doi.org/10.1016/j.ijantimicag.2020.106020.
36. Caniglia, J.L., Guda, M.R., Asuthkar, S., Tsung, A.J., and Velpula, K.K. (2020). A potential role for Galectin-3 inhibitors in the treatment of COVID-19. PeerJ. *8*. https://doi.org/10.7717/peerj.9392.
37. Nguyen, L., McCord, K.A., Bui, D.T., Bouwman, K.A., Kitova, E.N., Kumawat, D., Daskan, G.C., Tomris, I., Han, L., Chopra, P., et al. (2021). Sialic acid-dependent binding and viral entry of SARS-CoV-2. bioRRxiv. https://doi.org/10.1101/2021.03.08.434228.
38. Sun, X.-L. (2021). The role of cell surface sialic acids for SARS-CoV-2 infection. Glycobiology. https://doi.org/10.1093/glycob/cwab032.
39. Kwon, K.-C., and Daniell, H. (2016). Oral delivery of protein drugs bioencapsulated in plant cells. Mol. Ther. *24*, 1342–1350.

40. Chen, H., Li, Z., Zhang, L., Sawaya, P., Shi, J., and Wang, P. (2019). Quantitation of femtomolar-level protein biomarkers using a simple microbubbling digital assay and bright-field smartphone imaging. Angew. Chem. Int. Ed. *58*, 13922–13928.

41. Chen, H., Li, Z., Feng, S., Wang, A., Richard-Greenblatt, M., Hutson, E., Andrianus, S., Glaser, L., Rodino, K.G., Qian, J., et al. (2021). Femtomolar SARS-CoV-2 antigen detection using the microbubbling digital assay with smartphone readout enables antigen burden quantitation and dynamics tracking. medRxiv. https://doi.org/10.1101/2021.03.17.21253847.

42. Hoffmann, M., Kleine-Weber, H., Schroeder, S., Krüger, N., Herrler, T., Erichsen, S., Schiergens, T.S., Herrler, G., Wu, N.H., Nitsche, A., et al. (2020). SARS-CoV-2 cell entry depends on ACE2 and TMPRSS2 and is blocked by a clinically proven protease inhibitor. Cell *181*, 271–280.e8.

43. Daniell, H., Mangu, V., Yakubov, B., Park, J., Habibi, P., Shi, Y., Gonnella, P.A., Fisher, A., Cook, T., Zeng, L., et al. (2020). Investigational new drug enabling angiotensin oral-delivery studies to attenuate pulmonary hypertension. Biomaterials *233*. https://doi.org/10.1016/j.biomaterials.2019.119750.

44. Srinivasan, A., Herzog, R.W., Khan, I., Sherman, A., Bertolini, T., Wynn, T., and Daniell, H. (2021). Preclinical development of plant-based oral immune modulatory therapy for haemophilia B. Plant Biotechnol. J. *19*, 1952–1966. https://doi.org/10.1111/pbi.13608.

45. Daniell, H., Kulis, M., and Herzog, R.W. (2019). Plant cell-made protein antigens for induction of Oral tolerance. Biotechnol. Adv. *37*. https://doi.org/10.1016/j.biotechadv.2019.06.012.

46. Daniell, H., Jin, S., Zhu, X.G., Gitzendanner, M.A., Soltis, D.E., and Soltis, P.S. (2021). Green giant—a tiny chloroplast genome with mighty power to produce high-value proteins: history and phylogeny. Plant Biotechnol. J. *19*, 430–447.

47. Xu, H., Zhong, L., Deng, J., Peng, J., Dan, H., Zeng, X., Li, T., and Chen, Q. (2020). High expression of ACE2 receptor of 2019-nCoV on the epithelial cells of oral mucosa. Int. J. Oral Sci. *12*, 8.

48. Gary, E.N., Warner, B.M., Parzych, E.M., Griffin, B.D., Zhu, X., Tailor, N., Tursi, N.J., Chan, M., Purwar, M., Vendramelli, R., et al. (2021). A novel mouse AAV6 hACE2 transduction model of wild-type SARS-CoV-2 infection studied using synDNA immunogens. iScience *24*. https://doi.org/10.1016/j.isci.2021.102699.

49. Kirkeby, S. (2014). Cholera toxin B subunit-binding and ganglioside GM1 immunoexpression are not necessarily correlated in human salivary glands. Acta Odontol. Scand. *72*, 694–700.

50. Kirkeby, S., and Lynge Pedersen, A.M. (2018). Modifications of cholera toxin subunit B binding to human large intestinal epithelium. An immunohistochemical study. Microb. Pathogenesis *124*, 332–336.

51. Nowroozi, N., Kawata, T., Liu, P., Rice, D., and Zernik, J.H. (2001). High β-galactosidase and ganglioside GM1 levels in the human parotid gland. Arch. Otolaryngol. Head Neck Surg. *127*, 1381–1384.

52. Chen, L., Zhao, J., Peng, J., Li, X., Deng, X., Geng, Z., Shen, Z., Guo, F., Zhang, Q., Jin, Y., et al. (2020). Detection of 2019-nCoV in saliva and characterization of oral symptoms in COVID-19 patients. Cell Prolif. *53*. https://doi.org/10.1111/cpr.12923.

53. Xu, R., Cui, B., Duan, X., Zhang, P., Zhou, X., and Yuan, Q. (2020). Saliva: potential diagnostic value and transmission of 2019-nCoV. Int. J. Oral Sci. *12*, 11.

54. Xu, J., Li, Y., Gan, F., Du, Y., and Yao, Y. (2020). Salivary glands: potential reservoirs for COVID-19 asymptomatic infection. J. Dent Res. *99*, 989.

55. Liu, Y., Yan, L.M., Wan, L., Xiang, T.X., Le, A., Liu, J.M., Peiris, M., Poon, L.L., and Zhang, W. (2020). Viral dynamics in mild and severe cases of COVID-19. Lancet Infect. Dis. *20*, 656–657.

56. Batlle, D., Wysocki, J., and Satchell, K. (2020). Soluble angiotensin-converting enzyme 2: a potential approach for coronavirus infection therapy? Clin. Sci. *134*, 543–545.

57. Shenoy, V., Kwon, K.C., Rathinasabapathy, A., Lin, S., Jin, G., Song, C., Shil, P., Nair, A., Qi, Y., Li, Q., et al. (2014). Oral delivery of angiotensin-converting enzyme 2 and angiotensin-(1-7) bioencapsulated in plant cells attenuates pulmonary hypertension. Hypertension *64*, 1248–1259.

58. Peiris, J.S.M., Chu, C.M., Cheng, V.C.C., Chan, K.S., Hung, I.F.N., Poon, L.L., Law, K.I., Tang, B.S.F., Hon, T.Y.W., Chan, C.S., et al. (2003). Clinical progression and viral load in a community outbreak of coronavirus-associated SARS pneumonia: a prospective study. Lancet *361*, 1767–1772.

59. Sissoko, D., Duraffour, S., Kerber, R., Kolie, J.S., Beavogui, A.H., Camara, A.M., Colin, G., Rieger, T., Oestereich, L., Pályi, B., et al. (2017). Persistence and clearance of Ebola virus RNA from seminal fluid of Ebola virus disease survivors: a longitudinal analysis and modelling study. Lancet Glob. Health *5*, e80–e88.

60. Nagarajan, N., Yapp, E.K.Y., Le, N.Q.K., and Yeh, H.-Y. (2019). In silico screening of sugar alcohol compounds to inhibit viral matrix protein VP40 of Ebola virus. Mol. Biol. Rep. *46*, 3315–3324.

61. Berglund, J.P., Szczepanski, N., Penumarti, A., Beavers, A., Kesselring, J., Orgel, K., Burnett, B., Burks, A.W., and Kulis, M. (2017). Preparation and analysis of peanut flour used in oral immunotherapy clinical trials. J. Allergy Clin. Immunol. Pract. *5*, 1098–1104.

62. The PALISADE Group of Clinical Investigators (2018). AR101 oral immunotherapy for peanut allergy. N. Engl. J. Med. *379*, 1991–2001.

63. Park, J., Yan, G., Kwon, K.C., Liu, M., Gonnella, P.A., Yang, S., and Daniell, H. (2020). Oral delivery of novel human IGF-1 bioencapsulated in lettuce cells promotes musculoskeletal cell proliferation, differentiation and diabetic fracture healing. Biomaterials *233*. https://doi.org/10.1016/j.biomaterials.2019.119591.

64. Singh, R., Ren, Z., Shi, Y., Lin, S., Kwon, K.C., Shanmugaraj, B., Rai, V., Mante, F., Koo, H., and Daniell, H. (2021). Affordable oral health care: dental biofilm disruption using chloroplast made enzymes with chewing gum delivery. Plant Biotechnol. J. https://doi.org/10.1111/pbi.13643.

65. Yong, E.D.. Human Jaws Are Surprisingly Strong and Efficient. https://www.nationalgeographic.com/science/article/who-are-you-calling-weak-human-jaws-are-surprisingly-strong-and-efficient.

66. Takaki, P., Vieira, M., and Bommarito, S. (2014). Maximum bite force analysis in different age groups. Int. Arch. Otorhinolaryngol. *18*, 272–276.

67. Varga, S., Spalj, S., Lapter Varga, M., Anic Milosevic, S., Mestrovic, S., and Slaj, M. (2011). Maximum voluntary molar bite force in subjects with normal occlusion. Eur. J. Orthod. *33*, 427–433.

68. Guzzi, P.H., Mercatelli, D., Ceraolo, C., and Giorgi, F.M. (2020). Master regulator analysis of the SARS-CoV-2/human interactome. JCM *9*. https://doi.org/10.3390/jcm9040982.

69. Du, F., Liu, B., and Zhang, S. (2021). COVID-19: the role of excessive cytokine release and potential ACE2 down-regulation in promoting hypercoagulable state associated with severe illness. J. Thromb. Thrombolysis *51*, 313–329.

70. Ksenofontov, A.L., Badun, G.A., Fedorova, N.V., and Kordyukova, L.V. (2008). Quantitation of the glycoprotein spike area on the surface of enveloped viruses. Mol. Biol. *42*, 973–975.

71. Krammer, F., and Palese, P. (2015). Advances in the development of influenza virus vaccines. Nat. Rev. Drug Discov. *14*, 167–182.

72. Liu, Y.M., Shahed-Al-Mahmud, M., Chen, X., Chen, T.H., Liao, K.S., Lo, J.M., Wu, Y.M., Ho, M.C., Wu, C.Y., Wong, C.H., et al. (2020). A carbohydrate-binding protein from the edible lablab beans effectively blocks the infections of influenza viruses and SARS-CoV-2. Cell. Rep. *32*. https://doi.org/10.1016/j.celrep.2020.108016.

73. SeyedAlinaghi, S., Mirzapour, P., Dadras, O., Pashaei, Z., Karimi, A., MohsseniPour, M., Soleymanzadeh, M., Barzegary, A., Afsahi, A.M., Vahedi, F., et al. (2021). Characterization of SARS-CoV-2 different variants and related morbidity and mortality: a systematic review. Eur. J. Med. Res. *26*. https://doi.org/10.1186/s40001-021-00524-8.

74. Harvey, W.T., Carabelli, A.M., Jackson, B., Gupta, R.K., Thomson, E.C., Harrison, E.M., Ludden, C., Reeve, R., Rambaut, A., et al.; COVID-19 Genomics UK (COG-UK) Consortium (2021). SARS-CoV-2 variants, spike mutations and immune escape. Nat. Rev. Microbiol. *19*, 409–424.

75. Akkiz, H. (2021). Implications of the novel mutations in the SARS-CoV-2 genome for transmission, disease severity, and the vaccine development. Front. Med. *8*. https://doi.org/10.3389/fmed.2021.636532.

76. Hersh, E.V., Wolff, M., Moore, P.A., Theken, K.N., and Daniell, H. (2021). A pair of "ACEs". J. Dental Res. https://doi.org/10.1177/00220345211047510.

77. He, W., Baysal, C., Lobato Gómez, M., Huang, X., Alvarez, D., Zhu, C., Armario-Najera, V., Blanco Perera, A., Cerda Bennaser, P., Saba-Mayoral, A., et al. (2021). Contributions of international plant science community to fight against infectious diseases in human—part 2: affordable drugs in edible plants for endemic and re-emerging diseases. Plant Biotechnol. J. *19*, 1921–1936.